HHS Public Access

Author manuscript

ACS Chem Biol. Author manuscript; available in PMC 2016 May 17.

Published in final edited form as:

ACS Chem Biol. 2015 July 17; 10(7): 1718–1728. doi:10.1021/acschembio.5b00222.

Covalent Inhibition of Ubc13 Affects Ubiquitin Signaling and Reveals Active Site Elements Important for Targeting

Curtis D. Hodge[1], **Ross A. Edwards**[1], **Craig J. Markin**[1], **Darin McDonald**[2], **Mary Pulvino**[4], **Michael S. Y. Huen**[3], **Jiyong Zhao**[4], **Leo Spyracopoulos**[1], **Michael J. Hendzel**[2], and **J.N. Mark Glover**[1,*]

[1]Department of Biochemistry, University of Alberta, Edmonton, Alberta, Canada T6G 2H7

[2]Department of Oncology, University of Alberta, Edmonton, Alberta, Canada T6G 1Z2

[3]Department of Anatomy and Centre for Cancer Research, The University of Hong Kong, Hong Kong, China

[4]Department of Biomedical Genetics, University of Rochester, Rochester, New York, USA 14642

Abstract

Ubc13 is an E2 ubiquitin conjugating enzyme that functions in nuclear DNA damage signaling and cytoplasmic NF-κB signaling. Here we present the structures of complexes of Ubc13 with two inhibitors, NSC697923 and BAY 11-7082, which inhibit DNA damage and NF-κB signaling in human cells. NSC697923 and BAY 11-7082 both inhibit Ubc13 by covalent adduct formation through a Michael addition at the Ubc13 active site cysteine. The resulting adducts of both compounds exploit a binding groove unique to Ubc13. We developed a Ubc13 mutant which resists NSC697923 inhibition and, using this mutant, we show that the inhibition of cellular DNA damage and NF-κB signaling by NSC697923 is largely due to specific Ubc13 inhibition. We propose that unique structural features near the Ubc13 active site could provide a basis for the rational development and design of specific Ubc13 inhibitors.

Protein ubiquitination is a major post-translational system that regulates diverse aspects of eukaryotic intracellular signaling. The targeting of ubiquitin to specific proteins involves the initial ATP-dependent activation of ubiquitin by E1 enzymes that result in the thioester linkage of the C-terminal carboxylate of ubiquitin to the active site cysteine of the E1[1–4]. The activated ubiquitin is next transferred to the active site cysteine of any one of a number of ubiquitin conjugating enzymes (E2s), of which there are ~34 in the human genome[5, 6]. Most E2s function in cooperation with E3 proteins that bind and activate the E2 and recognize specific protein targets for ubiquitination[7–10].

*Corresponding author: Mark Glover, email: mark.glover@ualberta.ca.

Notes: The authors declare no competing financial interest.

Accession Codes

Ubc13~NSC697923: **4ONM**. Ubc13~BAY 11-7082: **4ONN**. $Ubc13^{QD}$: **4ONL**.

Supporting Information Available: This material is available free of charge via the Internet at http://pubs.acs.org.

The diverse effects of protein ubiquitination are driven in part by different forms of ubiquitin chains that can be linked to target proteins[11–13]. Chains in which the ε-amino group of Lys63 of one ubiquitin is joined to the C-terminal carboxylate of the next ubiquitin via an isopeptide bond (Lys63-linked chains) have been shown to play especially critical roles in NF-κB signaling[14–16] and the DNA damage response (DDR)[17, 18]. The formation of these chains is specifically catalyzed by a specialized ubiquitin conjugating enzyme (E2) complex composed of the canonical E2, Ubc13 (also known as Ube2N), together with one of either of two E2-like ubiquitin enzyme variant (Uev) proteins, Uev1a or Mms2 (also known as Ube2V1 and Ube2V2, respectively)[7, 19]. The Uev proteins bind the incoming acceptor ubiquitin, positioning its Lys63 for attack on the thioester of the donor ubiquitin covalently linked to the active site cysteine of Ubc13. The attack of the incoming lysine likely results in an oxyanion thioester intermediate that is thought to be stabilized by a conserved asparagine (Asn79 in Ubc13)[20]. This asparagine has also recently been implicated in maintaining the structural integrity of the Ubc13 active site loop (Ala114-Asp124)[21]. Further, substrate lysine pK_a suppression and deprotonation contribute to Ubc13 catalysis[22, 23].

The finding that the NF-κB pathway is constitutively activated in many forms of diffuse large B-cell lymphomas (DLBCLs) has driven efforts to develop small molecule inhibitors of this pathway. Recently, two independent reports[15, 16] have uncovered structurally related NF-κB inhibitors that biochemically target Ubc13. The first demonstrated that NSC697923 (2-[(4-methylphenyl)sulfonyl]-5-nitrofuran) inhibits Ubc13 and NF-κB activation, as well as the growth and survival of germinal center B-cell-like and activated B-cell-like DLBCLs[16]. In addition, this compound was also shown to inhibit ubiquitin-dependent DNA damage signaling but not DNA damage-induced γH2AX foci formation, consistent with the specific targeting of Ubc13 in the nucleus. Another compound, BAY 11-7082 ((2*E*)-3-[(4-methylphenyl)sulfonyl]prop-2-enenitrile), previously thought to be a protein kinase inhibitor[24], has also been shown to inhibit Ubc13 through covalent modification of the active site cysteine[15]. BAY 11-7082 was shown to inhibit not only Ubc13 but also other E2 enzymes as well as the proteasome. In contrast, NSC697923 was found to be specific for Ubc13 in *in vitro* ubiquitination assays[16], suggesting that this compound might provide a more attractive lead toward the development of a targeted Ubc13 agent.

Here, we present the structures of Ubc13 inhibited by both NSC697923 and BAY 11-7082. The structures reveal that both inhibitors act via the covalent modification of the active site cysteine through a Michael addition[15]. Interestingly, the cysteine adduct docks into an adjacent cleft that is not present in many other ubiquitin conjugating enzymes. To examine the role of this cleft in inhibition, we created a Ubc13 mutant in which the cleft is obscured by a change in the active site loop to a conformation that resembles that observed in the NSC697923-resistant homologue, UbcH5c. We show that the mutant is competent to build Lys63-linked polyubiquitin chains and is resistant to NSC697923 inhibition, but not to BAY 11-7082. Using this mutant, we conclusively demonstrate that inhibition of DNA damage and NF-κB signaling by NSC697923 in mammalian cells is primarily due to Ubc13 inhibition. Our approach provides a means for future development of NSC697923 derivatives that exploit the unique Ubc13 binding cleft while alleviating overall cellular

toxicity. Further, novel Ubc13 inhibitors can more effectively be discovered through the use of the mutant as a counter screen to identify compounds that exploit the unique Ubc13 binding cleft.

RESULTS and DISCUSSION

Ubc13 Covalent Inhibitors Bind to a Groove near the Active Site

To understand how NSC697923 and BAY 11-7082 interact with and inhibit Ubc13, we determined the crystal structures of these compounds bound to Ubc13/Mms2 (Figure 1a-e). NSC697923 reacts with the sulfhydryl group of Cys87 through a Michael addition (Figure 1f), resulting in the addition of a 5-nitrofuran moiety to the Cys87 sulfur atom (Figure 1b and Supporting Information Figure 1a,b). NSC697923 also reacts with the free sulfhydryl of β-mercaptoethanol in a pH-dependent reaction that can be monitored via absorbance at 380 nm (Supporting Information Figure 2a,b). The 5-nitrofuran group is packed into a cleft leading to Cys87, the walls of which are composed of the residue 114–124 loop on one side, and the residue 81–85 turn on the other side (Supporting Information Figure 2c). The packing of this group within the cleft is largely hydrophobic with a single hydrogen bond between the nitro group and the side chain of Asn123. The conformation of Ubc13 is largely unchanged by reaction with the inhibitor, except for a 1.8 Å shift of Cys87 to accommodate the 5-nitrofuran.

Similarly, BAY 11-7082 reacts with the sulfhydryl group of Cys87 through a Michael addition[15] (Figure 1f), which leaves a prop-2-enenitrile moiety on the Cys87 sulfur atom (Figure 1d and Supporting Information Figure 2d). The electron density shows that the prop-2-enenitrile adduct is directed toward Asn123 forming a hydrogen bond, positioned within the same groove as the 5-nitrofuran moiety of the NSC697923 complex. The electron density suggests that there may also be a proportion of Ubc13 in these crystals which are unmodified or where the adduct is disordered (Supporting Information Figure 2d). As in the NSC697923 complex, there is little movement of residues in the BAY 11-7082 structure compared to the uninhibited structure; however, unlike the NSC697923 complex, there is no shift in the main chain near Cys87 induced by reaction with the BAY 11-7082 inhibitor (Figure 1e).

The two inhibitors are similar in that they both contain a tosyl group that is released as a result of the reaction (Figure 1f). We wondered if the tosyl group might also play a role in the initial binding of the inhibitors prior to reaction. We tested the ability of NSC697923 to bind to a nonreactive Ubc13 mutant containing a Cys-Ser substitution at the active site by NMR. Comparison of the ^{15}N HSQC spectra of the C87S mutant incubated with 250 mM NSC697923 compared to a Ubc13^{C87S} + DMSO control revealed no significant shifts in any backbone amides, suggesting there is little if any specific prereaction binding of the compound near the active site (Supporting Information Figure 3a).

Development of an Inhibitor-Resistant Ubc13 Mutant

Previous work suggested UbcH5c is resistant to NSC697923 *in vitro*, under concentrations that effectively inhibit Ubc13[16]. Comparison of the structures of Ubc13 and UbcH5c suggests a mechanism for this differential sensitivity to the inhibitor (Figure 2a,b). The

groove that the nitrofuran substituent occupies in Ubc13 is occupied by a conserved leucine (Leu119) in UbcH5c. While an analogous leucine is present in Ubc13 (Leu121), this leucine is solvent exposed due to a different conformation of the 114–124 loop. An alignment of Ubc13 with the 17 available structurally similar catalytically active E2 structures in humans indicates that in the other E2s this loop often adopts the UbcH5c-like conformation with a residue frequently occluding the groove, providing a possible explanation for the specificity of NSC697923 for Ubc13 (Supporting Information Figure 3b). The other seven available E2 enzyme structures show considerable divergence from this basic fold (Supporting Information Figure 3c).

Analysis of the Ubc13 and UbcH5c structures and amino acid sequence alignments (Figure 2a,b), suggests that four amino acid substitutions might flip the orientation of the loop and alter the character of the groove adjacent to the Ubc13 active site, which could render the mutant resistant to NSC697923. Two of the mutations in the 114–124 loop, A122V and N123P, were predicted to alter the loop conformation, orienting Leu121 into the groove, while also shifting the position of Asn123, the sole hydrogen bonding partner for the nitrofuran. The other two mutations, D81N and R85S, were designed to alter the wall of the groove opposite the 114–124 loop to resemble UbcH5c. The crystal structure of the quadruple Ubc13 mutant ($Ubc13^{QD}$) bound to Mms2 reveals that the 114–124 loop does adopt a UbcH5c-like conformation such that Leu121 occupies the groove to potentially occlude the inhibitor (Figure 2c–e).

$Ubc13^{QD}$ Is Resistant to NSC697923 but not BAY 11-7082

We next compared the sensitivities of the $Ubc13^{QD}$ mutant and wild type Ubc13 to inhibition using *in vitro* ubiquitination assays that contained stoichiometric amounts of the E3 RNF8, which stimulates Mms2/Ubc13-dependent formation of Lys63-linked polyubiquitin chains[7] (Figure 3a,b). Reactions performed in the absence of inhibitor reveal that the $Ubc13^{QD}$ mutant is competent to build Lys63-linked poly-ubiquitin chains (Supporting Information Figure 4), and chain building efficiency under these reaction conditions is very similar to wild type. As seen in Figure 3a, Lys63-linked polyubiquitination catalyzed by wild type Ubc13 is inhibited by NSC697923 concentrations as low as 1 μM, consistent with previous findings[16]. In contrast, polyubiquitination catalyzed by $Ubc13^{QD}$ is not markedly inhibited at similar concentrations of NSC697923. While these results reveal a significant resistance of the $Ubc13^{QD}$ mutant to NSC697923, both $Ubc13^{WT}$ and $Ubc13^{QD}$ are similarly inhibited by BAY 11-7082 (Figure 3b). The fact that $Ubc13^{QD}$ is highly sensitive to BAY 11-7082 but not NSC697923 suggests that the smaller BAY 11-7082 is able to evade the more restricted environment of the $Ubc13^{QD}$ active site. This is consistent with previous results that indicate that BAY 11-7082 is able to inhibit ubiquitination catalyzed by a range of E2s, many of which adopt a 114–124 loop conformation that is very similar to that of the $Ubc13^{QD}$ mutant[15].

These results suggest that the $Ubc13^{QD}$ mutant reacts more slowly than the wild type protein with NSC697923. To directly test this, we used the finding that reaction of NSC697923 with sulfhydryl compounds can be followed by the formation of a reaction product that absorbs UV light at 380 nm (Supporting Information Figure 2a,b). We used this assay to quantitate

the rate of reaction of NSC697923 with Ubc13^{QD} compared to the wild type protein (Figure 3c). Fitting of the data to a second order kinetic model gives a second order rate constant (k_2) for the reaction with wild type Ubc13 of 410 ± 102 $M^{-1}s^{-1}$, whereas reaction with Ubc13^{QD} is ~16-fold slower (k_2 of 26 ± 8 $M^{-1}s^{-1}$). No reaction was observed in control experiments with the catalytically inactive Ubc13^{C87S}.

Inhibition of the DDR and NF-κB Signaling by NSC697923 is Due to Targeting of Ubc13

Our development of a functional Ubc13 variant that is resistant to NSC697923 presented the opportunity to test if the ability of NSC697923 to inhibit the cellular DNA damage response and NF-κB signaling is due to inhibition of Ubc13 or an off-target effect. In these experiments, we utilized a Ubc13 knockout mouse embryonic fibroblast line (MEF) in which we reintroduced either wild type Ubc13 or Ubc13^{QD}, Supporting Information Figure 5. NF-κB activation was induced by treatment with lipopolysaccharide (LPS) and monitored by following the cellular localization of the NF-κB p65 subunit, which translocates from the cytoplasm to the nucleus upon I-κB degradation in a manner that depends on the action of Uev1a/Ubc13[25]. In the absence of inhibitor, both wild type and Ubc13^{QD} are able to induce nearly total translocation of p65 to the nucleus upon LPS stimulation (Figure 4a) and consistent with previous findings this translocation is greatly dependent upon Ubc13 (Supporting Information Figure 6a,b)[26]. Treatment of WT reconstituted MEF cells with 2.5 μM NSC697923 inhibited the LPS-driven translocation of p65, so that a large amount remained in the cytoplasm. Treatment of Ubc13^{QD} reconstituted MEFs with 2.5 μM NSC697923 resulted in less overall inhibition (Figure 4b). These treatments did not significantly alter p65 expression in the MEF cell lines (Supporting Information Figure 6c). Quantification of these results reveals that the average percentage of total p65 localized to the nucleus is reduced from 51 ± 1% to 33 ± 1% upon treatment with 2.5 μM NSC697923 in WT cells (Figure 4b,c). Given that ~30% of p65 is localized to the nucleus in these cells in the absence of NF-κB activation, this represents an almost complete inhibition of LPS-inducible NF-κB signaling. In contrast, in Ubc13^{QD} cells, the average percentage of nuclear p65 is only reduced from 51 ± 1% to 39 ± 1% upon NSC697923 treatment, which is well above the level of p65 translocation in the absence of LPS treatment (~30%). We find that this reflects a statistically significant reduction in inhibition in Ubc13^{QD} compared to Ubc13^{WT} cells (P-value = 0.02), and thus, the effects of NSC697923 on NF-κB signaling are likely due, at least in part, to Ubc13 inhibition (Figure 4c).

To further assess the effect of NSC697923 on NF-κB signaling, we also analyzed the cellular cytokine release profile of the MEF cell lines (Figure 5) in response to LPS stimulation. Cytokines are small secreted signaling proteins that are extensively used by cells of the immune system, in particular macrophages, for intercellular communication and inflammation regulation in response to foreign particles/invaders[27]. As a major component of the connective tissue, fibroblasts are also known to secrete cytokines in response to stimulation via other cytokines or LPS[27, 28]. We found four cytokines that were responsive to LPS stimulation in a Ubc13-dependent manner suggesting that their expression levels are largely controlled by the NF-κB pathway in our cells (Supporting Information Figure 7). We measured the levels of these secreted cytokines as a function of increasing NSC697923 concentration (Figure 5 and Supporting Information Figure 8). The NSC697923-dependent

reduction of the four cytokines, granulocyte-colony stimulating factor (G-CSF), monocyte chemoattractant protein 1 (MCP-1), granulocyte-macrophage-colony stimulating factor (GM-CSF), and interleukin-5 (IL-5) [27–30], was slightly more pronounced in the wild type cells compared to the Ubc13^{QD} cells. This is most notable when comparing the cytokine concentration differences between the DMSO control and the lower NSC697923 concentrations (0.5 to 2 μM) as seen in the normalized data in Figure 5 (raw data in Supporting Information Figure 8). The longer incubation with NSC697923 (4.5 h) and the complex nature of the pathways contributing to cytokine secretion may explain the lower sensitivity of this experiment compared to the p65 translocation data (a more direct measure of NF-κB signaling). Taken together, however, the cytokine secretion data are consistent with the p65 translocation data, which suggests that the effects on the NF-κB signaling pathway are partially due to Ubc13 inhibition.

We utilized the same MEF cell lines to monitor the effects of NSC697923 on the cellular response to DNA damage signaling. DNA damage was induced with ionizing radiation and DNA lesions were monitored through the formation of γH2AX foci, which form independent of Ubc13-dependent ubiquitin signaling[31, 32]. In the Ubc13 knockout MEFs, we observed a slight increase in γH2AX foci upon ionizing radiation, which was decreased upon treatment with NSC697923, however neither effect was statistically significant (Supporting Information Figure 9a,b). To assess downstream signaling, we monitored the formation of 53BP1 foci, which are dependent on Ubc13 driven ubiquitination of chromatin[33, 34] (Figure 6a-c, Supporting Information Figure 9b). In both the wild type- and Ubc13^{QD}-expressing cells, we observed the colocalization of γH2AX and 53BP1 foci in response to ionizing radiation, indicating that the Ubc13^{QD} mutant is competent to functionally replace the wild type protein in the DNA damage response. It should be noted that there was a small (not statistically significant) increase in colocalization of γH2AX and 53BP1 (i.e., DNA damage) in the absence of ionizing radiation for both WT and QD cell lines upon treatment with NSC697923 (Supporting Information Figure 9c). This may be attributed to the reaction of NSC697923 with the natural cellular antioxidant glutathione, which could result in an increase in DNA damaging reactive oxygen species (ROS). Treatment of the irradiated cells with 2.5 μM NSC697923 did not alter the appearance of the γH2AX foci, but did significantly reduce the percentage of cells positive for colocalized γH2AX/53BP1 foci in wild type Ubc13-expressing cells (P-value = 9.0^{-9}; Figure 6a,c). There was no statistically significant inhibition of the γH2AX/53BP1 colocalized-positive Ubc13^{QD}-expressing cells (P-value = 0.7) indicating that the effect of NSC697923 on the DNA damage response is largely due to the inhibition of Ubc13 (Figure 6b,c).

Ubc13 is the ubiquitin-conjugating (E2) enzyme critical for the synthesis of Lys63-linked ubiquitin chains in both the homologous recombination DNA repair and NF-κB pathways, which have both been identified as targets for cancer therapy development. Here we have shown that two previously identified inhibitors of Ubc13 both covalently modify the active site cysteine, forming sulfur adducts that dock into a unique groove adjacent to the catalytic cysteine. This groove is occluded by a loop opposing the active site cysteine in many E2 enzymes and therefore provides a route for the development of specific inhibitors of Ubc13. Mutations that block this groove but do not significantly impair catalytic activity afford

resistance to one of the inhibitors *in vitro*. Using this resistant mutant, we show that the previously demonstrated inhibition of NF-κB and DNA damage signaling attributed to this compound is predominantly due to the specific inhibition of Ubc13. However, we do note that the mutant only provides a partial reduction in the inhibition of the NF-κB response. This raises the possibility that NSC697923, which is generally reactive to small molecule sulfhydryl compounds, may act on alternative targets that also inhibit the NF-κB pathway.

A comparison of the structure of free Ubc13 with the structure of Ubc13 with a ubiquitin covalently linked to the active site indicates that a UbcH5c-like conformation can be induced in the Ubc13 114–124 loop upon ubiquitin binding[19] (Supporting Information Figure 10). The ubiquitin-bound structure provides a view of the covalently bound donor ubiquitin, as well as an incoming acceptor ubiquitin (Figure 7). In the unbound state, Leu121 blocks the approach of the incoming lysine from the acceptor ubiquitin, however rearrangement of the 114–124 loop enables the access of ubiquitin Lys63 to the active site. This conformational rearrangement also shifts the position of Ubc13 Asn123, which, in the free state, is hydrogen bonded to the main chain of His77, Pro78 and Val80. Upon ubiquitin binding and conformational change, Asn123 flips out and hydrogen bonds with the main chain of Lys63 of the acceptor ubiquitin and the adjacent Gln62 residue. The fact that an asparagine is only found at this position in Ubc13 among all the 34 known active human E2 enzymes suggests that this conformational rearrangement may be unique to Ubc13 (Supporting Information Figure 11). Flexibility of this loop is further suggested by the observation that the loop adopts still other conformations in complex with E3 ligases and other regulatory proteins (Supporting Information Figure 12). Indeed, we have recently shown the dynamics of this loop to be important for the catalytic activity of Ubc13[35]. This is consistent with previous suggestions that E3 ligases may activate Ubc13 and other E2s by driving conformational change within the active site that propagates from the site of E3 binding[8, 9, 36].

NSC697923 and BAY 11-7082 provide a starting point for future development of agents that act to covalently inhibit Ubc13. While covalent inhibitors were rarely utilized in the past for targeted drug discovery, many important drugs in current use act through a covalent mechanism, and there is renewed interest in covalent inhibitors[37]. A key to lowering the toxicity of such inhibitors is to modulate their reactivity, so that their activation and reaction with a target is dependent upon stable and selective binding. Our work shows that the groove near the active site of Ubc13 can serve as a powerful selectivity determinant. The charged Asp119 near the active site could also be exploited as a hydrogen bond/salt bridge acceptor. Replacement of the nitro group in NSC697923 could offer a route to reduce the reactivity of the inhibitor, while potentially alleviating the well-known toxicities associated with nitrofuran-containing compounds[38]. Our NMR experiments do not demonstrate specific prereaction binding of NSC697923 to $Ubc13^{C87S}$, arguing against the idea that the tosyl group, which is common to both inhibitors, directly contributes to Ubc13 binding. Nevertheless, next generation inhibitors could employ leaving groups that might enhance the precatalytic binding of the inhibitor to Ubc13. Interestingly, the predicted position of the tosyl group would be close to a groove that accepts the ubiquitin tail in E2-ubiquitin

complex structures[8, 19], and it is therefore possible that leaving groups or other modifications that target this groove could significantly improve binding.

BAY 11-7082 has been extensively used in studies of the NF-κB pathway, and recently been shown to target protein tyrosine phosphatases[15, 39]. It has previously been demonstrated that BAY 11-7082 is toxic to multiple myeloma cells independent of its known effects on the NF-κB pathway, indicating off-target effects[40]. This study did not, however, take into account the more recent report of the inhibition of protein tyrosine phosphatases by this compound[39]. We found that the Ubc13^{QD} mutant was not resistant to BAY 11-7082, despite the predicted clash of Leu121 with the prop-2-enenitrile moiety. The smaller prop-2-enenitrile adduct may not dock as well into the active site pocket as the larger nitrofuran, and may exhibit greater mobility to evade the steric clash with Leu121. The ability of the Ubc13^{QD} mutant to discriminate between a bulkier, more specific compound and a smaller, more promiscuous one speaks to its potential utility as an effective active site binding inhibitor counter-screen.

In principle, noncovalent, allosteric inhibition could provide another route for the development of therapeutically useful Ubc13-targeted compounds. While E2 enzymes in general lack the deep, complex active site clefts that characterize traditionally druggable targets, an allosteric inhibitor of another E2 enzyme, Cdc34, has been developed[41]. The Cdc34 inhibitor, CC0651, binds and induces a conformational change in Cdc34 that opens the enzyme structure to accommodate the inhibitor and also distorts the active site to inhibit Cdc34 catalytic activity. The authors suggest that this pocket could be exploited to develop similar inhibitors specific to a variety of different E2 enzymes, including Ubc13.

The importance of developing specific inhibitors of a critical, nonredundant enzyme such as Ubc13 that plays essential roles in pathways that are intimately associated with tumour cell viability and susceptibility to treatments cannot be underestimated. A recent study has shown Ubc13 to be among a number of genes that have increased expression in nasopharyngeal carcinoma cells resistant to cisplatin, which display a greater frequency of sister chromatid exchange via template switching[42]. Depletion of Ubc13 in these cells suppresses sister chromatid exchange and resensitizes these cells to cisplatin. Another recent study demonstrated that increased Uev1A levels can drive human breast cancer cell invasion and metastasis in mouse xenograft models in a manner that is dependent on Ubc13[43]. Ubc13 has also been shown to control breast cancer metastasis through the activation of a TAK1-p38 kinase[44]. Chronic inflammation is often a precursor to cancer development, and the NF-κB pathway is often constitutively activated in many cancers, which can, in part, lead to acquired chemo-resistance[45]. An effective Ubc13 inhibitor could target chemo-resistant cancer cells through inhibition of the Ubc13-dependent template switching and NF-κB pathways, aid in breast cancer metastasis prevention, and sensitize these cells to DNA damaging radiation/chemotherapy through inhibition of the Ubc13-dependent DDR.

METHODS

Protein production

Ubc13, Mms2, RNF8, and mUBA1 cloning, and protein production/purification was previously described[7, 46, 47]. Further details described in Supporting Information.

Crystallization and structure determination

The $Ubc13^{WT}$ (or $Ubc13^{QD}$)/Mms2 heterodimeric complexes were mixed with either NSC697923 (NCI) or BAY11-7082 (Sigma) and incubated overnight at 4 °C prior to setting up crystallization trials. Data were collected and the structures were refined. Detailed preparation of crystallization conditions are described in Supporting Information.

Ubiquitination inhibition assay

When necessary mUBA1, Ubc13 (WT or QD), Mms2, RNF8, ubiquitin, and ATP were added, and allowed to react for 1.5 hours at 37 °C. Reactions were quenched with SDS-PAGE loading buffer and visualized by Western blotting. The primary antibody was mouse anti-ubiquitin (Santa Cruz, sc-166553) and the secondary was goat antimouse-FITC (Sigma-Aldrich). Further reaction details described in Supporting Information.

In vitro inhibition absorbance assay

NSC697923 was added to the various Ubc13 constructs and the absorbance at 380 nm was monitored via a Synergy MX Biotek plate reader. The second-order rate constants were determined as described in Supporting Information.

NMR of $^{15N}Ubc13^{C87S}$ and NSC697923

NSC697923 in DMSO or DMSO alone was added to ^{15}N labeled $Ubc13^{C87S}$, and chemical shift changes were monitored by NMR spectroscopy using 2D ^{1}H-^{15}N HSQC spectra. Supporting Information contains additional details.

Assay for NF-κB signaling and DNA damage localization in MEFs

MEF cells were seeded to ~$8.57x10^4$ the day before using a hemocytometer. MEFs were incubated with NSC697923 for 30 minutes prior to either LPS stimulation or ionizing radiation treatment. Cells were fixed using 4 % paraformaldehyde and stained with either an anti-p65 antibody (Santa Cruz, sc-372), or anti-53BP1 (Santa Cruz, sc-22760) and anti-γH2AX (Millipore, 05–636) antibodies. Invitrogen (37–1100) anti-Ubc13 antibody was used for Western blotting. MetaMorph was used to acquire single-plane images. Images were independently scaled in Photoshop CS3 (Adobe) for Windows, to best represent the subcellular distribution of the fluorescent stain. Further technical details are described in Supporting Information.

Multiplex Mouse Cytokine Array

MEF conditioned medium was assayed by Eve Technologies (Calgary, Alberta, Canada) using Multiplexing LASER bead technology. Briefly the method entails the addition of different coloured fluorescent beads coupled with specific cytokine-specific antibodies to

the medium, which can be discriminated via a bead analyzer. A biotinylated antibody is used to detect the cytokine, which is then quantified using a fluorescent streptavidin-phycoerythrin conjugate. The target analyte is directly proportional to the amount of conjugate detected by the bead analyzer. For a full list of cytokines analyzed see the Supporting Information.

CellProfiler and Statistical Analyses

CellProfiler was used to find and measure nuclei, cytoplasm, and foci of the MEF cells in the 16-bit TIFF files, for which the Otsu thresholding method was chosen[48–50]. Statistical significance was determined using a two-tailed Student's *t* test and significance level of *P<0.05 (unless otherwise specified) using Microsoft Excel 2010.

Supplementary Material

Refer to Web version on PubMed Central for supplementary material.

Acknowledgments

The authors thank P. Grochulski, K. Janzen, and M. Fodje at the Canadian Light Source and S. Classen at the Advanced Light Source (SIBYLS) for crystallographic data collections support. They also thank the Flow Cytometry Units and Cellular Imaging Facility at the Cross Cancer Institute for the use of flow cytometers and microscopes and S. Baksh for helpful discussions. This work was performed with support from Canadian Cancer Society/Canadian Breast Cancer Research Alliance (to J.N.M.G.), the Canadian Institutes of Health Research (CIHR114975 to J.N.M.G.; CIHR119515 to M.J.H.), the National Institutes of Health (CA92584 to J.N.M.G.), and the Alberta Innovates Health Solutions.

References

1. Haas AL, Siepmann TJ. Pathways of ubiquitin conjugation. FASEB J. 1997; 11:1257–1268. [PubMed: 9409544]
2. Hershko A, Ciechanover A. The ubiquitin system. Annu Rev Biochem. 1998; 67:425–479. [PubMed: 9759494]
3. Pickart CM, Eddins MJ. Ubiquitin: structures, functions, mechanisms. Biochim Biophys Acta. 2004; 1695:55–72. [PubMed: 15571809]
4. Dye BT, Schulman BA. Structural mechanisms underlying posttranslational modification by ubiquitin-like proteins. Annu Rev Biophys Biomol Struct. 2007; 36:131–150. [PubMed: 17477837]
5. Michelle C, Vourc'h P, Mignon L, Andres CR. What was the set of ubiquitin and ubiquitin-like conjugating enzymes in the eukaryote common ancestor? J Mol Evol. 2009; 68:616–628. [PubMed: 19452197]
6. van Wijk SJ, Timmers HT. The family of ubiquitin-conjugating enzymes (E2s): deciding between life and death of proteins. FASEB J. 2010; 24:981–993. [PubMed: 19940261]
7. Campbell SJ, Edwards RA, Leung CC, Neculai D, Hodge CD, Dhe-Paganon S, Glover JN. Molecular insights into the function of RING finger (RNF)-containing proteins hRNF8 and hRNF168 in Ubc13/Mms2-dependent ubiquitylation. J Biol Chem. 2012; 287:23900–23910. [PubMed: 22589545]
8. Plechanovova A, Jaffray EG, Tatham MH, Naismith JH, Hay RT. Structure of a RING E3 ligase and ubiquitin-loaded E2 primed for catalysis. Nature. 2012; 489:115–120. [PubMed: 22842904]
9. Pruneda JN, Littlefield PJ, Soss SE, Nordquist KA, Chazin WJ, Brzovic PS, Klevit RE. Structure of an E3:E2~Ub complex reveals an allosteric mechanism shared among RING/U-box ligases. Mol Cell. 2012; 47:933–942. [PubMed: 22885007]
10. Lu CS, Truong LN, Aslanian A, Shi LZ, Li Y, Hwang PY, Koh KH, Hunter T, Yates JR 3rd, Berns MW, Wu X. The RING finger protein RNF8 ubiquitinates Nbs1 to promote DNA double-strand

break repair by homologous recombination. J Biol Chem. 2012; 287:43984–43994. [PubMed: 23115235]

11. Komander D, Rape M. The ubiquitin code. Annu Rev Biochem. 2012; 81:203–229. [PubMed: 22524316]
12. Markin CJ, Xiao W, Spyracopoulos L. Mechanism for recognition of polyubiquitin chains: balancing affinity through interplay between multivalent binding and dynamics. J Am Chem Soc. 2010; 132:11247–11258. [PubMed: 20698691]
13. Sato Y, Yoshikawa A, Mimura H, Yamashita M, Yamagata A, Fukai S. Structural basis for specific recognition of Lys 63-linked polyubiquitin chains by tandem UIMs of RAP80. EMBO J. 2009; 28:2461–2468. [PubMed: 19536136]
14. Iwai K. Diverse ubiquitin signaling in NF-kappaB activation. Trends Cell Biol. 2012; 22:355–364. [PubMed: 22543051]
15. Strickson S, Campbell DG, Emmerich CH, Knebel A, Plater L, Ritorto MS, Shpiro N, Cohen P. The anti-inflammatory drug BAY 11-7082 suppresses the MyD88-dependent signalling network by targeting the ubiquitin system. Biochem J. 2013; 451:427–437. [PubMed: 23441730]
16. Pulvino M, Liang Y, Oleksyn D, DeRan M, Van Pelt E, Shapiro J, Sanz I, Chen L, Zhao J. Inhibition of proliferation and survival of diffuse large B-cell lymphoma cells by a small-molecule inhibitor of the ubiquitin-conjugating enzyme Ubc13-Uev1A. Blood. 2012; 120:1668–1677. [PubMed: 22791293]
17. Mailand N, Bekker-Jensen S, Faustrup H, Melander F, Bartek J, Lukas C, Lukas J. RNF8 ubiquitylates histones at DNA double-strand breaks and promotes assembly of repair proteins. Cell. 2007; 131:887–900. [PubMed: 18001824]
18. Doil C, Mailand N, Bekker-Jensen S, Menard P, Larsen DH, Pepperkok R, Ellenberg J, Panier S, Durocher D, Bartek J, Lukas J, Lukas C. RNF168 binds and amplifies ubiquitin conjugates on damaged chromosomes to allow accumulation of repair proteins. Cell. 2009; 136:435–446. [PubMed: 19203579]
19. Eddins MJ, Carlile CM, Gomez KM, Pickart CM, Wolberger C. Mms2-Ubc13 covalently bound to ubiquitin reveals the structural basis of linkage-specific polyubiquitin chain formation. Nat Struct Mol Biol. 2006; 13:915–920. [PubMed: 16980971]
20. Wu PY, Hanlon M, Eddins M, Tsui C, Rogers RS, Jensen JP, Matunis MJ, Weissman AM, Wolberger C, Pickart CM. A conserved catalytic residue in the ubiquitin-conjugating enzyme family. EMBO J. 2003; 22:5241–5250. [PubMed: 14517261]
21. Berndsen CE, Wiener R, Yu IW, Ringel AE, Wolberger C. A conserved asparagine has a structural role in ubiquitin-conjugating enzymes. Nat Chem Biol. 2013; 9:154–156. [PubMed: 23292652]
22. Markin CJ, Saltibus LF, Kean MJ, McKay RT, Xiao W, Spyracopoulos L. Catalytic proficiency of ubiquitin conjugation enzymes: balancing pK(a) suppression, entropy, and electrostatics. J Am Chem Soc. 2010; 132:17775–17786. [PubMed: 21114314]
23. Yunus AA, Lima CD. Lysine activation and functional analysis of E2-mediated conjugation in the SUMO pathway. Nat Struct Mol Biol. 2006; 13:491–499. [PubMed: 16732283]
24. Pierce JW, Schoenleber R, Jesmok G, Best J, Moore SA, Collins T, Gerritsen ME. Novel Inhibitors of Cytokine-induced I B Phosphorylation and Endothelial Cell Adhesion Molecule Expression Show Anti-inflammatory Effects in Vivo. J Biol Chem. 1997; 272:21096–21103. [PubMed: 9261113]
25. Andersen PL, Zhou H, Pastushok L, Moraes T, McKenna S, Ziola B, Ellison MJ, Dixit VM, Xiao W. Distinct regulation of Ubc13 functions by the two ubiquitin-conjugating enzyme variants Mms2 and Uev1A. J Cell Biol. 2005; 170:745–755. [PubMed: 16129784]
26. Wertz IE, Dixit VM. Signaling to NF-kappaB: regulation by ubiquitination. Cold Spring Harb Perspect Biol. 2010; 2:a003350. [PubMed: 20300215]
27. Arango Duque G, Descoteaux A. Macrophage cytokines: involvement in immunity and infectious diseases. Front Immunol. 2014; 5:491. [PubMed: 25339958]
28. Huleihel M, Douvdevani A, Segal S, Apte RN. Different regulatory levels are involved in the generation of hemopoietic cytokines (CSFs and IL-6) in fibroblasts stimulated by inflammatory products. Cytokine. 1993; 5:47–56. [PubMed: 8485305]

29. Takatsu K. Revisiting the identification and cDNA cloning of T cell-replacing factor/interleukin-5. Front Immunol. 2014; 5:639. [PubMed: 25566252]
30. Teferedegne B, Green MR, Guo Z, Boss JM. Mechanism of action of a distal NF-kappaB-dependent enhancer. Mol Cell Biol. 2006; 26:5759–5770. [PubMed: 16847329]
31. Fernandez-Capetillo O, Lee A, Nussenzweig M, Nussenzweig A. H2AX: the histone guardian of the genome. DNA Repair (Amst). 2004; 3:959–967. [PubMed: 15279782]
32. Lukas J, Lukas C, Bartek J. Mammalian cell cycle checkpoints: signalling pathways and their organization in space and time. DNA Repair (Amst). 2004; 3:997–1007. [PubMed: 15279786]
33. Huen MS, Huang J, Yuan J, Yamamoto M, Akira S, Ashley C, Xiao W, Chen J. Noncanonical E2 variant-independent function of UBC13 in promoting checkpoint protein assembly. Mol Cell Biol. 2008; 28:6104–6112. [PubMed: 18678647]
34. Fradet-Turcotte A, Canny MD, Escribano-Diaz C, Orthwein A, Leung CC, Huang H, Landry MC, Kitevski-LeBlanc J, Noordermeer SM, Sicheri F, Durocher D. 53BP1 is a reader of the DNA-damage-induced H2A Lys 15 ubiquitin mark. Nature. 2013; 499:50–54. [PubMed: 23760478]
35. Rout MK, Hodge CD, Markin CJ, Xu X, Glover JN, Xiao W, Spyracopoulos L. Stochastic gate dynamics regulate the catalytic activity of ubiquitination enzymes. J Am Chem Soc. 2014; 136:17446–17458. [PubMed: 25423605]
36. Soss SE, Klevit RE, Chazin WJ. Activation of UbcH5c~Ub is the result of a shift in interdomain motions of the conjugate bound to U-box E3 ligase E4B. Biochemistry. 2013; 52:2991–2999. [PubMed: 23550736]
37. Singh J, Petter RC, Baillie TA, Whitty A. The resurgence of covalent drugs. Nat Rev Drug Discov. 2011; 10:307–317. [PubMed: 21455239]
38. Vass M, Hruska K, Franek M. Nitrofuran antibiotics: a review on the application, prohibition and residual analysis. Vet Med-Czech. 2008; 53:469–500.
39. Krishnan N, Bencze G, Cohen P, Tonks NK. The anti-inflammatory compound BAY-11-7082 is a potent inhibitor of protein tyrosine phosphatases. FEBS J. 2013; 280:2830–2841. [PubMed: 23578302]
40. Rauert-Wunderlich H, Siegmund D, Maier E, Giner T, Bargou RC, Wajant H, Stuhmer T. The IKK inhibitor Bay 11-7082 induces cell death independent from inhibition of activation of NFkappaB transcription factors. PloS one. 2013; 8:e59292. [PubMed: 23527154]
41. Ceccarelli DF, Tang X, Pelletier B, Orlicky S, Xie W, Plantevin V, Neculai D, Chou YC, Ogunjimi A, Al-Hakim A, Varelas X, Koszela J, Wasney GA, Vedadi M, Dhe-Paganon S, Cox S, Xu S, Lopez-Girona A, Mercurio F, Wrana J, Durocher D, Meloche S, Webb DR, Tyers M, Sicheri F. An allosteric inhibitor of the human Cdc34 ubiquitin-conjugating enzyme. Cell. 2011; 145:1075–1087. [PubMed: 21683433]
42. Su WP, Hsu SH, Wu CK, Chang SB, Lin YJ, Yang WB, Hung JJ, Chiu WT, Tzeng SF, Tseng YL, Chang JY, Su WC, Liaw H. Chronic treatment with cisplatin induces replication-dependent sister chromatid recombination to confer cisplatin-resistant phenotype in nasopharyngeal carcinoma. Oncotarget. 2014; 5:6323–6337. [PubMed: 25051366]
43. Wu Z, Shen S, Zhang Z, Zhang W, Xiao W. Ubiquitin-conjugating enzyme complex Uev1A-Ubc13 promotes breast cancer metastasis through nuclear factor-small ka, CyrillicB mediated matrix metalloproteinase-1 gene regulation. Breast Cancer Res. 2014; 16:R75. [PubMed: 25022892]
44. Wu X, Zhang W, Font-Burgada J, Palmer T, Hamil AS, Biswas SK, Poidinger M, Borcherding N, Xie Q, Ellies LG, Lytle NK, Wu LW, Fox RG, Yang J, Dowdy SF, Reya T, Karin M. Ubiquitin-conjugating enzyme Ubc13 controls breast cancer metastasis through a TAK1-p38 MAP kinase cascade. Proc Natl Acad Sci U S A. 2014; 111:13870–13875. [PubMed: 25189770]
45. Crawford S. Is it time for a new paradigm for systemic cancer treatment? Lessons from a century of cancer chemotherapy. Front Pharmacol. 2013; 4:68. [PubMed: 23805101]
46. Moraes TF, Edwards RA, McKenna S, Pastushok L, Xiao W, Glover JN, Ellison MJ. Crystal structure of the human ubiquitin conjugating enzyme complex, hMms2-hUbc13. Nat Struct Biol. 2001; 8:669–673. [PubMed: 11473255]

47. Carvalho AF, Pinto MP, Grou CP, Vitorino R, Domingues P, Yamao F, Sa-Miranda C, Azevedo JE. High-yield expression in Escherichia coli and purification of mouse ubiquitin-activating enzyme E1. Mol Biotechnol. 2012; 51:254–261. [PubMed: 22012022]

48. Carpenter AE, Jones TR, Lamprecht MR, Clarke C, Kang IH, Friman O, Guertin DA, Chang JH, Lindquist RA, Moffat J, Golland P, Sabatini DM. CellProfiler: image analysis software for identifying and quantifying cell phenotypes. Genome Biol. 2006; 7:R100. [PubMed: 17076895]

49. Kamentsky L, Jones TR, Fraser A, Bray MA, Logan DJ, Madden KL, Ljosa V, Rueden C, Eliceiri KW, Carpenter AE. Improved structure, function and compatibility for CellProfiler: modular high-throughput image analysis software. Bioinformatics. 2011; 27:1179–1180. [PubMed: 21349861]

50. Sezgin M, Sankur B. Survey over image thresholding techniques and quantitative performance evaluation. J Electron Imaging. 2004; 13:146–168.

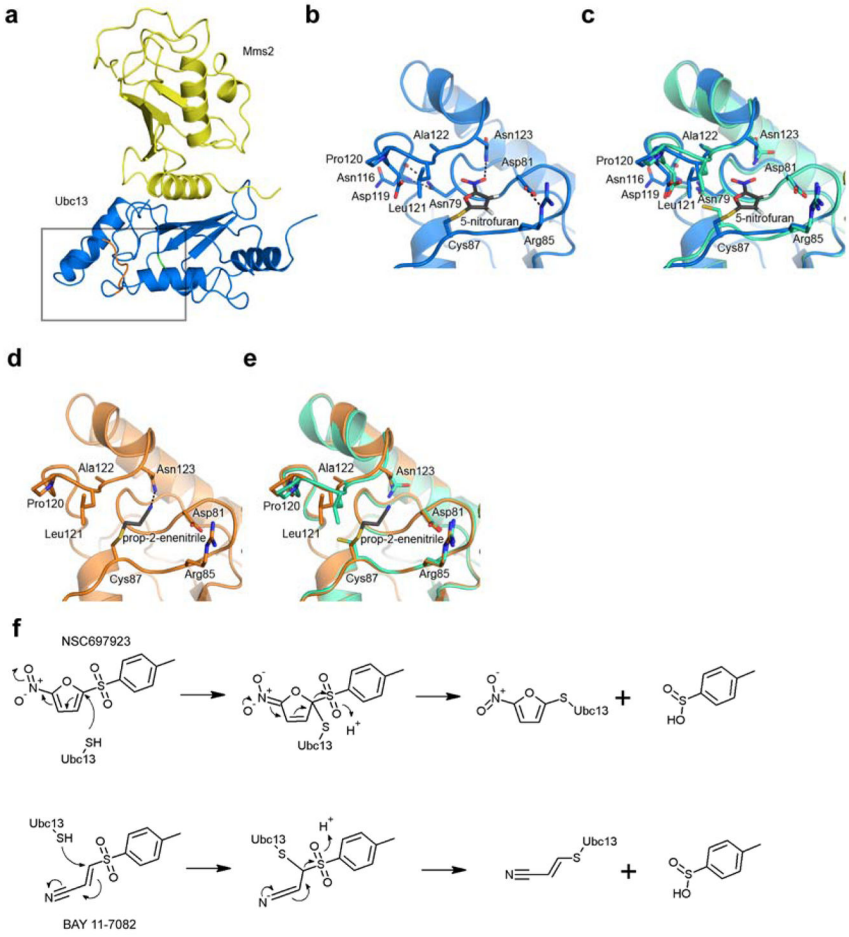

Figure 1.

NSC697923 and BAY 11-7082 covalently modify the Ubc13 active site. (a) Overview of Ubc13 (blue)/Mms2 (yellow) bound by the 5-nitrofuran moiety of NSC697923. Active site is boxed with the 114–124 loop in orange and the Cys87 region in green (Protein Data Bank accession 4ONM). (b) The active site view of Ubc13 bound by the 5-nitrofuran moiety of NSC697923. (c) Overlay of wild type Ubc13, PDB 1J7D (green-cyan), and 5-nitrofuran-bound Ubc13. (d) Active site view of Ubc13 bound by the prop-2-enenitrile moiety of BAY 11-7082 (PDB 4ONN). (e) Overlay of wild type Ubc13 and prop-2-enenitrile bound Ubc13. In panels (b) – (e), the view is rotated 90° from the orientation in (a). (f) Mechanisms of covalent attachment by NSC697923 and BAY 11-7082.

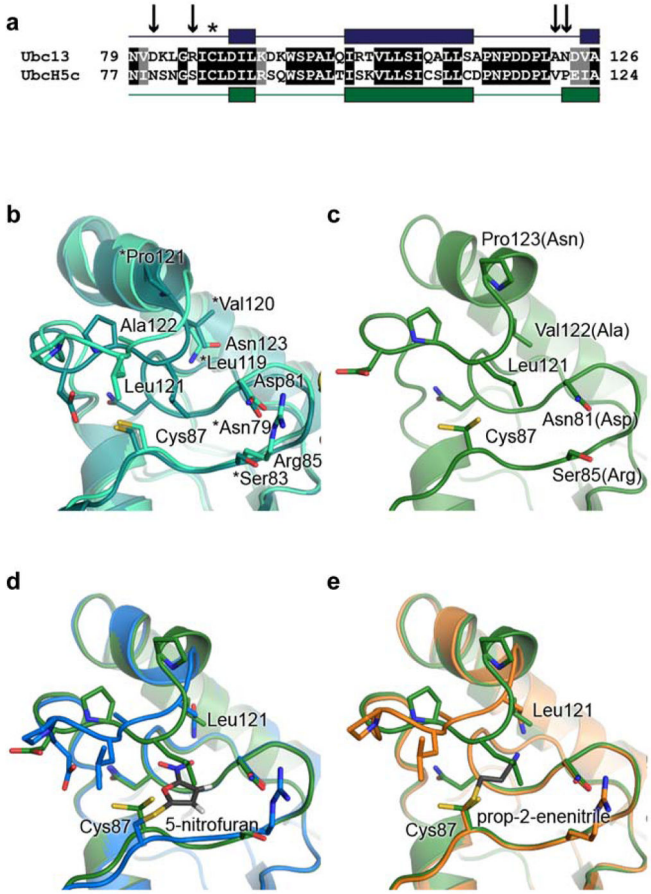

Figure 2.

Design and structure of a NSC697923 resistant Ubc13 mutant. (a) Amino acid sequence alignment of important active site residues in Ubc13 and UbcH5c, with secondary structural characteristics shown above. A line signifies a loop region and a box denotes an α helix. Arrows indicate mutations made to Ubc13 to mimic UbcH5c. The asterisk is above the active site cysteine. (b) Overlay of UbcH5c, PDB 1X23 (deep-teal), and Ubc13 (light green) shows their different active site loop conformations. Asterisks denote UbcH5c residues. (c) Active site view of the mutant $Ubc13^{QD}$ (green) with the UbcH5c-type loop conformation (PDB 4ONL). Brackets denote wildtype residues. (d) Overlay of Ubc13 5-nitrofuran adduct (blue) and the resistant $Ubc13^{QD}$ (green). (e) Overlay of Ubc13 prop-2-enenitrile adduct (orange) and $Ubc13^{QD}$.

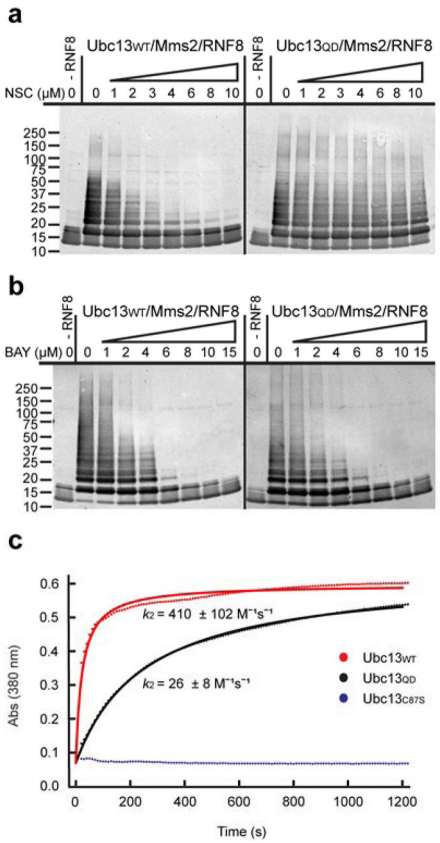

Figure 3.

Ubc13^{QD} is resistant to NSC697923 but not BAY 11-7082. (a and b) *In vitro* ubiquitination assays in which purified Ubc13/Mms2 (Ubc13^{WT} or Ubc13^{QD}) was incubated with ubiquitin, ATP, E1 enzyme, RNF8 and the indicated concentrations of inhibitor. Results were visualized by Western blotting with an antiubiquitin antibody. (a) Results for NSC697923. (b) Results for BAY 11-7082. (c) Representative graph of an *in vitro* inhibition assay monitored by absorbance at 380 nm. Reactions containing either Ubc13^{WT}, Ubc13^{QD}, or Ubc13^{C87S} were mixed with the NSC697923 inhibitor, and the resulting absorbance monitored. The experiment was done in triplicate and the average second-order rate constants (k_2) and standard errors are reported. Dotted lines indicate experimental data, curves indicate the fit to a second-order rate model.

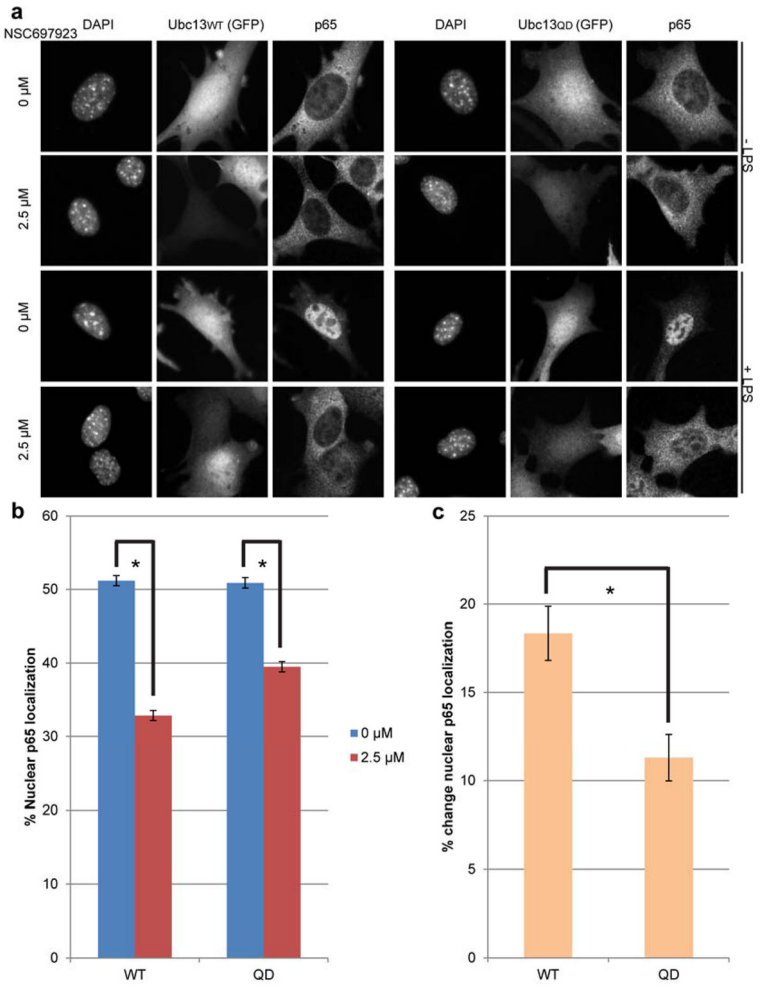

Figure 4.

Inhibition of Ubc13 is required for significant disruption of cellular NF-κB signaling by NSC697923. (a) Representative images of $Ubc13^{WT}$ (left) or $Ubc13^{QD}$ (right) reconstituted mouse embryonic fibroblast cells before and after lipopolysaccharide (LPS) stimulation, with and without NSC697923 treatment (2.5 μM). (b) Quantitation of p65 translocation represented as a percent of intensity localized to the nuclei and (c) the difference in p65 translocation between NSC697923-untreated and treated cells (P-value = 0.02). Unstimulated cells have approximately 30% background nuclear p65 translocation. Data from three independent experiments were pooled with at least 200 cells per condition, and standard error of image averages is included. The tonal range of whole images was rescaled from 0 to 255 in Photoshop to increase the overall contrast for display.

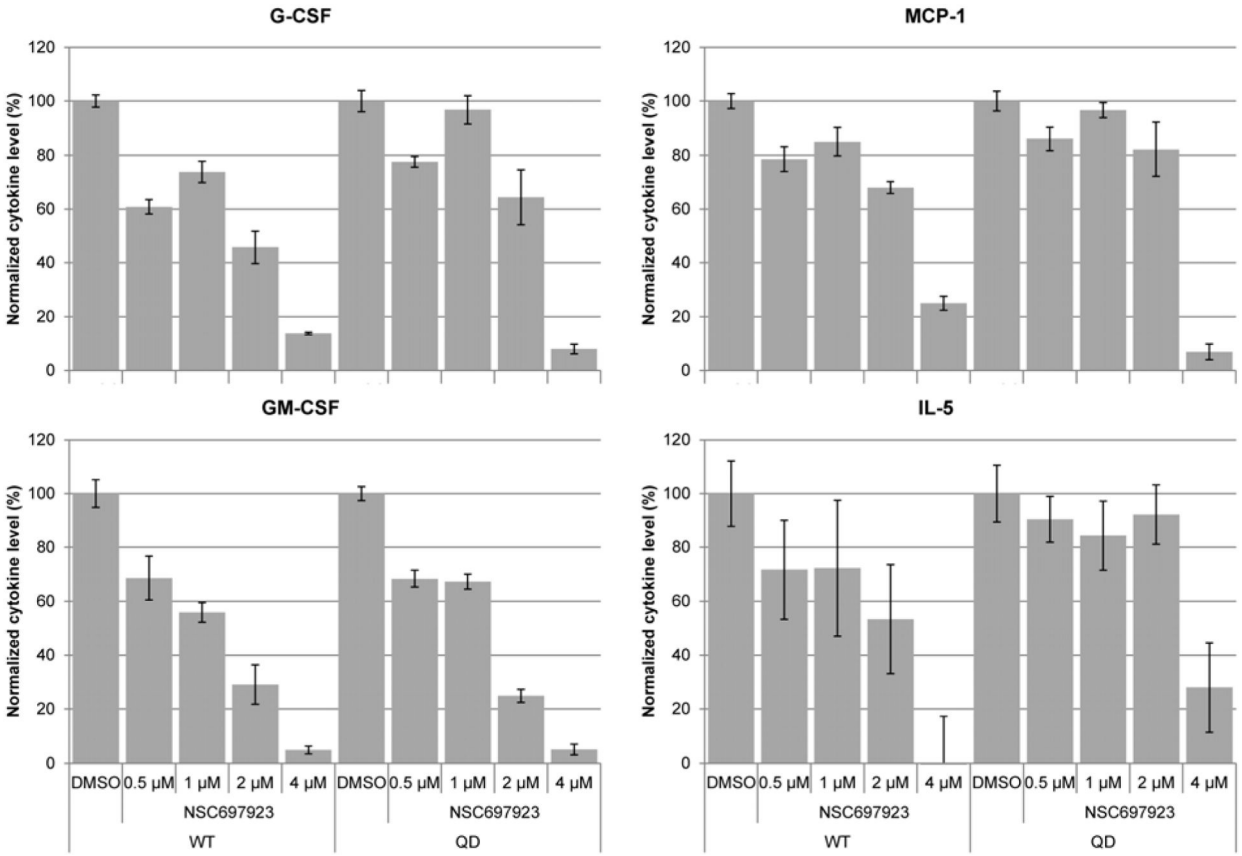

Figure 5.

Normalized inhibition of Ubc13-dependent, NF-κB-driven cytokine release by NSC697923. Unstimulated (−LPS) or stimulated (+LPS) $Ubc13^{WT}$ or $Ubc13^{QD}$ MEF cells were treated with either DMSO, or increasing concentrations of NSC697923 from 0.5 μM to 4 μM and cytokine levels in the culture medium were quantified. The background unstimulated (−LPS) level was subtracted from each treatment (DMSO to 4 μM NSC697923) and the stimulated (+LPS) DMSO treated level was normalized to 100% for optimal direct comparison of the two cell lines. The assay was done in triplicate, and the standard error of the mean for each treatment is included.

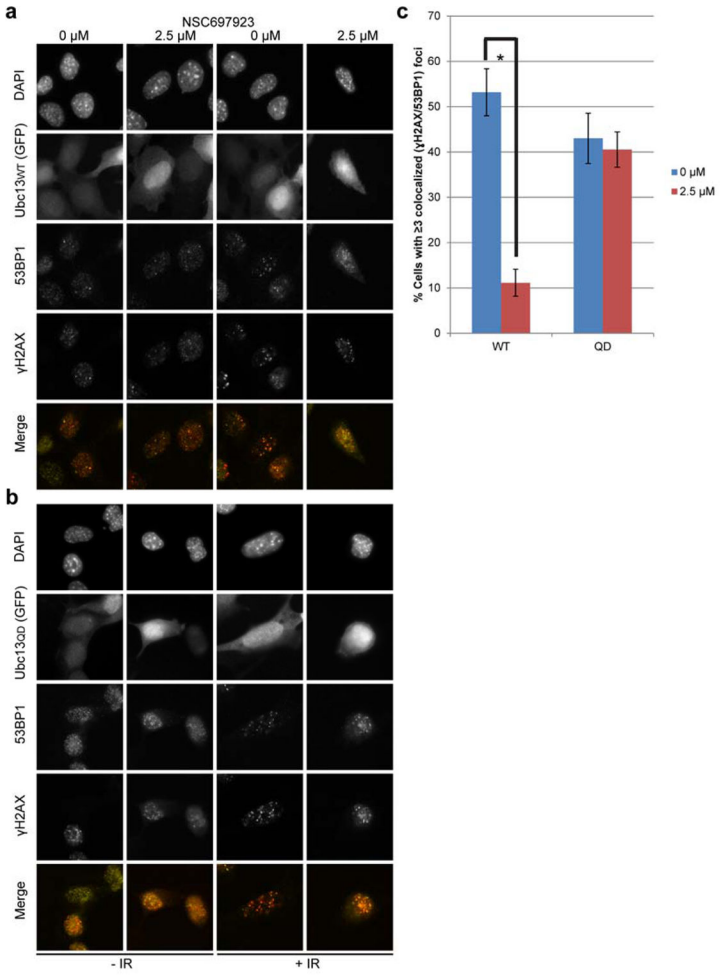

Figure 6.

Inhibition of Ubc13 is required for disruption of cellular DNA damage signaling by NSC697923. (a) Representative images of $Ubc13^{WT}$ or (b) $Ubc13^{QD}$ reconstituted mouse embryonic fibroblast cells plus/minus 3 Gy of ionizing radiation, with or without NSC697923 treatment (2.5 μM). (c) Quantitation of 53BP1 localization represented as a percentage of total cells positive (≥3 foci) for γH2AX/53BP1 colocalization. Data from three independent experiments were pooled with at least 300 cells per condition, and standard error of image averages is included. The tonal range of whole images was rescaled from 0 to 255 in Photoshop to increase the overall contrast for display.

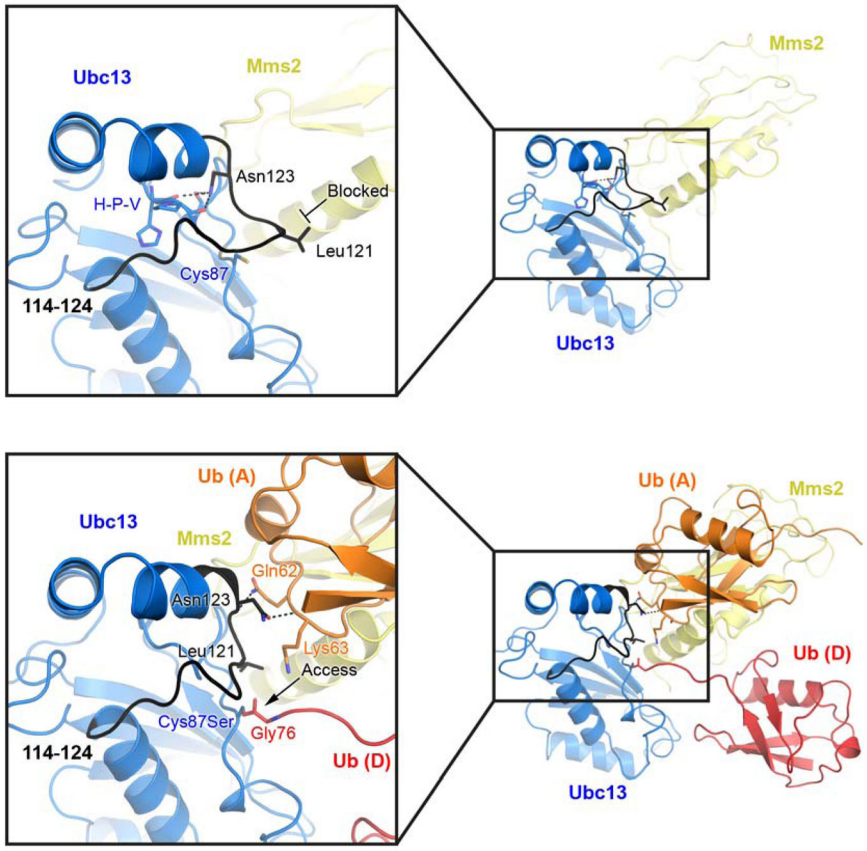

Figure 7.

Conformational changes in Ubc13 loop 114–124 upon ubiquitin binding. The top panel is hUbc13/hMms2 (PDB 1J7D) and the bottom panel is yUbc13~hUb/yMms2/hUb (2GMI). Ubc13 is blue, Mms2 is yellow, donor ubiquitin is red, and acceptor ubiquitin is orange for both panels and the 114–124 loop is in black. The position of Leu121 in the unbound structure (top panel) is expected to block the approach of Lys63 of the acceptor ubiquitin toward the active site cysteine